RSC Advances

PAPER

View Article Online
View Journal | View Issue

Cite this: *RSC Adv.*, 2021, **11**, 23631

A strategy for preparing controllable, superhydrophobic, strongly sticky surfaces using SiO_2@PVDF raspberry core–shell particles†

Seung-Hyun Kim, Hong Suk Kang, Eun-Ho Sohn, Bong-Jun Chang, In Jun Park and Sang Goo Lee *

In nature, wetting by water droplets on superhydrophobic materials is governed by the Cassie–Baxter or Wenzel models. Moreover, sticky properties, derived from these types of wettings, are required for a wide range of applications involving superhydrophobic materials. As a facile new strategy, a method employing a gaseous fluorine precursor to fabricate core–shell particles, comprising perfectly shaped fluorine shells with adjustable adhesive strength, is described in this paper. Silica was used as the hydrophilic core, while polyvinylidene fluoride (PVDF) was used for the hydrophobic shell coating, forming a raspberry-like shape. In addition, controlling the amount of PVDF coated on the silica surface enabled the water droplets to come into contact with both the PVDF of the shell and the silica of the core, thereby controlling both the superhydrophobicity and the adhesive strength. Thus, the synthesized particles formed a structured coating with controllable stickiness and contact angles of 131–165°. Furthermore, on surfaces with high adhesivity, the water droplets remained stable at tilt angles of 90° and 180° even under a strong centrifugal force, whereas on surfaces with low adhesivity, the water droplets slid off when the substrate was tilted at 4°.

Received 20th May 2021
Accepted 30th June 2021

DOI: 10.1039/d1ra03928h

rsc.li/rsc-advances

1. Introduction

In recent years, biomimetic superhydrophobic surfaces have garnered considerable attention in the field of liquid/solid interfaces. A superhydrophobic surface has a water droplet contact angle (CA) greater than 150°, while the water droplets roll or slide off the surface at an inclination angle of less than 5°.[1] These surfaces exhibit the characteristic lotus effect, corresponding to the Cassie–Baxter wetting state.[2] Typically, superhydrophobic surfaces that exhibit the lotus effect have been used for oil/water separation, reducing friction, increasing thermal stability, increasing transparency, and *in vivo* drug release, and in self-cleaning, antibacterial, anti-fogging, anti-icing, and anti-contamination surfaces.[3–15] However, in applications like microdrop manipulation, water harvesting, microfluidic transportation, chemical/biological separation, microanalysis, and *in situ* detection, a sticky surface is necessary.[16–22] This is generally achieved using the rose petal effect, which corresponds to the Wenzel wetting state.[23] Such surfaces are fabricated by chemical etching, plasma treatment, photolithography, chemical vapor deposition, chemical coating, and using colloidal particles.[24–30]

The structured colloidal coatings have high CAs because the area of solids and gases in the contact region between the droplet and the structured surface can be easily controlled.[31,32] Furthermore, the CA can be adjusted according to the empty space between the particles.[33,34] In particular, raspberry-shaped particles have a larger volume of empty space than normal particles, which results in a larger water CA.[35,36] Additionally, the surface modification of colloidal particles with fluorine groups have significantly low free energy, thus yielding a structured coating with a larger CA.[37,38] Although this strategy provides a large CA, it does not produce a sticky surface. In contrast, certain raspberry-shaped particles provide adhesivity owing to the van der Waals forces or the large amount of space between them. However, this adhesivity is difficult to control.[39,40]

To obtain a structured coating with a high CA and controllable high-strength adhesivity, we describe the fabrication of SiO_2@PVDF raspberry core–shell particles (SPRCSPs) by coating polyvinylidene fluoride (PVDF) onto SiO_2 particles. Unlike silica

Interface Materials and Chemical Engineering Research Center, Korea Research Institute of Chemical Technology, Daejeon, 34114, Republic of Korea. E-mail: sgoo@krict.re.kr

† Electronic supplementary information (ESI) available: Additional TEM images of SPRCSPs prepared using VDF gas (VDF 10, 15, and 18 g) (Fig. S1); XPS spectra and SEM images of SPRCSPs (VDF 25 g) (Fig. S2); a schematic illustration and optical image for measuring the CA, and SEM images of PVDF and SPRCSPs (VDF 25 g) (Fig. S3); schematic of a moving water drop on an SPRCSP ordered structure (Fig. S4); videos of the dropping behavior and movement of the water droplets on a sticky structured coating of SPRCSPs (VDF 15 g, Video S1) and SPRCSPs (VDF 18 g, Video S2); video of a moving water droplet dropped onto a SPRCSP (VDF 18 g) structured coating at a tilting angle of 4° (Video S3). See DOI: 10.1039/d1ra03928h

particles that have been surface-modified using fluorine compounds, the current approach offers perfect control over the SPRCSPs shell thickness. Previously, a liquid precursor has been used to prepare the shell of the raspberry-shaped core–shell particles.[41] However, to the best of our knowledge, this is the first study to report perfect raspberry-shaped inorganic@organic core–shell particles directly prepared using a gaseous precursor, *viz.* 1,1-difluoroethylene (VDF). Our SPRCSPs exhibit high CAs ranging from 131 to 165°, depending on the degree of PVDF coating. In addition, they have controllable, strong adhesive properties owing to the high electronegativity of fluorine and hydrophilicity of the silica surface. In addition, the adhesivity of the coating was controllable, which ensured that the water droplets remained on the coating surface even under a strong centrifugal force at tilt angles of 90° and 180° (vertical and upside down, respectively), while they slid off at a tilt angle of 4°.

2. Materials and methods

2.1 Materials

We used the following materials as received: tetraethyl orthosilicate (TEOS, 98.0%, Sigma-Aldrich), an ammonium hydroxide solution (NH_4OH, 28–30%, Sigma-Aldrich), 3-(trimethoxysilyl) propyl methacrylate (TPM, 98%, Sigma-Aldrich), 1,1-difluoroethylene VDF (Apollo Scientific), and ammonium persulfate (APS, >98.0%, Sigma-Aldrich).

2.2. Methods

2.2.1 Synthesis of SiO_2 particles. SiO_2 colloidal particles were prepared using the Stöber method. Typically, deionized (DI) water (30 mL) was added to ethanol (EtOH, 500 mL) and mixed at 1000 rpm for 30 min. Next, NH_4OH (28–30 wt%, 30 mL) was added to the solution and mixed for 20 min. Then, TEOS (30 mL) was added to the solution and stirred at 1000 rpm for 6 h at room temperature (25 °C). Finally, TPM (6 mL) was added, and the mixture was stirred for 6 h. After this sol–gel process, the unreacted precursors were removed by washing with EtOH.

2.2.2 Preparation of SiO_2@PVDF raspberry core–shell particles (SPRCSPs). The SPRCSPs were synthesized *via* emulsion polymerization. Typically, the SiO_2 colloidal particles were diluted to 5 wt% in DI water. Then, this SiO_2 particle suspension (5 mL) was added to DI water (100 mL) inside a 500 mL stainless steel autoclave jacket at 25 °C; subsequently, the jacket was closed. After degassing, the solution was heated to 82 °C and mixed at 300 rpm. Next, an initiator solution consisting of APS (0.125 g) and DI water (3 mL) was injected into the jacket. Finally, 10–25 g of VDF was continuously injected while maintaining the pressure at 15.0 bar.

2.2.3 Preparation of SiO_2@PVDF raspberry core–shell particle structured coatings. The SPRCSP structured coatings were prepared using a simple, convenient method of spray-coating the SPRCSP solution (10 wt% in EtOH) onto a cover glass. The solvent was then removed by evaporation at room temperature (25 °C).

2.3 Characterization

The colloidal particles and structured coatings were observed *via* scanning electron microscopy (SEM, Hitachi, S-4300) and transmission electron microscopy (TEM, FEI Talos F200X) to determine their size and morphology, respectively. TEM with energy-dispersive X-ray spectroscopy (EDS, FEI Talos F200X) mapping was conducted to identify the distributions of Si, O, and F. The modifications to the silica particles were identified by Fourier-transform infrared (FT-IR) spectroscopy (FT/IR-4100, JASCO). The chemical compositions were analyzed using X-ray photoelectron spectroscopy (XPS, ESCALAB 250) and the CAs were measured using an optical goniometer (DSA 100, Krüss) with 6 μL water droplets. The sliding angle was measured using high-speed cameras (HiSpec1 4G Color, Fastec Imaging Co., Ltd).

3. Results and discussion

3.1 Preparation of SiO_2@PVDF raspberry core–shell particles

To create a structured coating with controllable sticky superhydrophobicity with respect to water, the SPRCSPs were fabricated using hydrophilic silica particles as the core, and coating them with the hydrophobic PVDF raspberry-shaped shell (Fig. 1a). First, the SiO_2 spherical particles were prepared as uniform-sized cores (Fig. 1b) using a sol–gel method. Owing to the presence of OH groups on their surface, PVDF cannot be directly coated onto the silica particles as a shell. Thus, the particle surfaces were first functionalized with vinyl groups and the resulting vinyl-functionalized silica particles (V-SiO_2) were dispersed in ethanol to prevent agglomeration.[42,43] However, unlike other polymers, PVDF particles must be synthesized from a gaseous precursor rather than a liquid. Therefore, the presence of even a small amount of ethanol may interfere with the reaction and prevent the synthesis. Hence, the silica surface must be further modified to facilitate the mixing of the OH and vinyl groups. Thus, 3-(trimethoxysilyl)propyl methacrylate (TPM) was added prior to fully growing the silica particles from tetraethyl orthosilicate (TEOS). As a result, the desired surface modification was obtained using a facile one-pot approach instead of the conventional method, where the synthesized silica particles are first cleaned, followed by the surface modification with TPM. Based on the FT-IR peaks at 1740 and 3040 cm^{-1} (Fig. 1c), the prepared particles contained C=O and CH=CH_2 bonds. This indicates that the PVDF coating formed a raspberry-like surface (Fig. 1d and e) because the OH and vinyl groups were mixed on the surface of the silica. Furthermore, the EDS elemental mapping images showed that the core had a uniform distribution of Si and O, while the PVDF shell coating had a uniform distribution of F (Fig. 1f–h).

The stickiness of the raspberry particles can be attributed to the large gaps between the particles[44] and the van der Waals forces.[40] To obtain controllable and strong adhesivity, we exploited the advantageous properties of the conventional raspberry-like particles. Accordingly, we controlled the degree of the shell coating to enable the interaction of water with the core, thereby enabling Wenzel wetting. Thus, water-dispersible (instead of ethanol) V-SiO_2 particles were first prepared, which

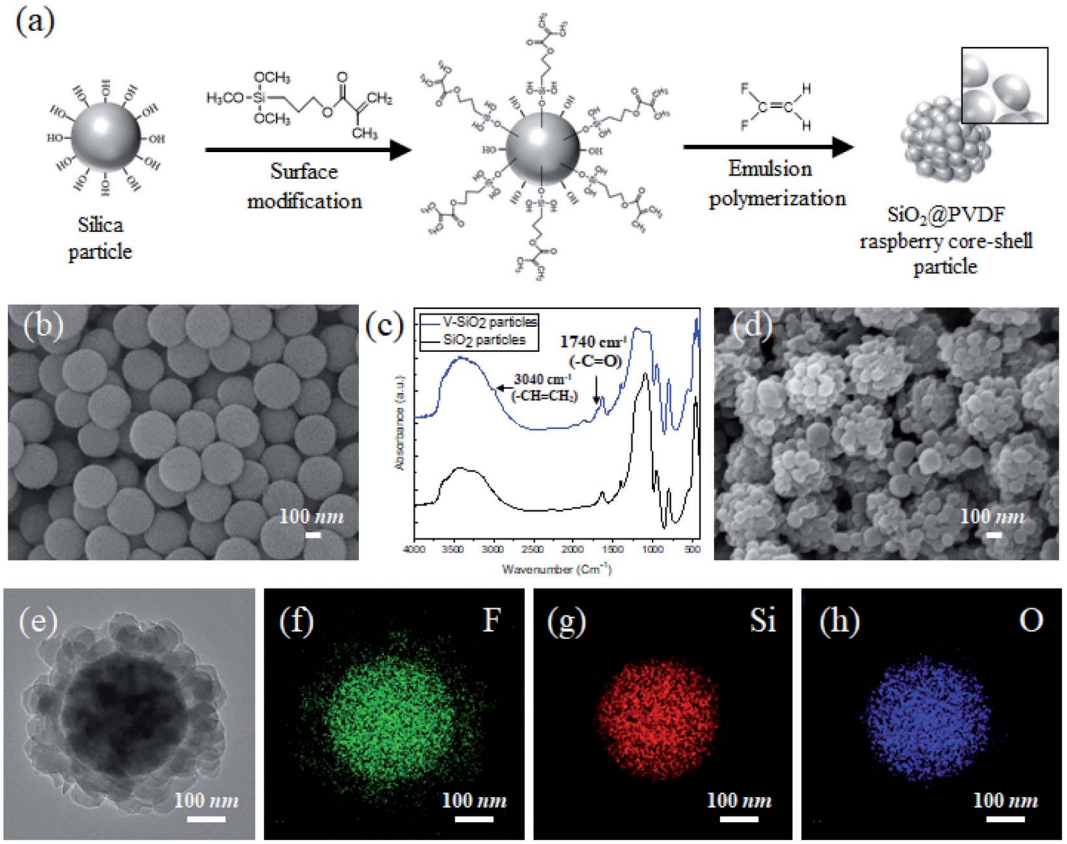

Fig. 1 Preparation and analysis of SPRCSPs. (a) Schematic of SPRCSP preparation, including the synthetic route to produce SPRCSPs from SiO_2 spheres functionalized by vinyl groups through emulsion polymerization of VDF precursors into PVDF. (b) SEM images of V-SiO_2 particles. (c) FT-IR spectra of SiO_2 and V-SiO_2 particles. (d) SEM and (e) TEM images of SPRCSPs. (f–h) EDS elemental mappings of F, Si, and O of SPRCSPs.

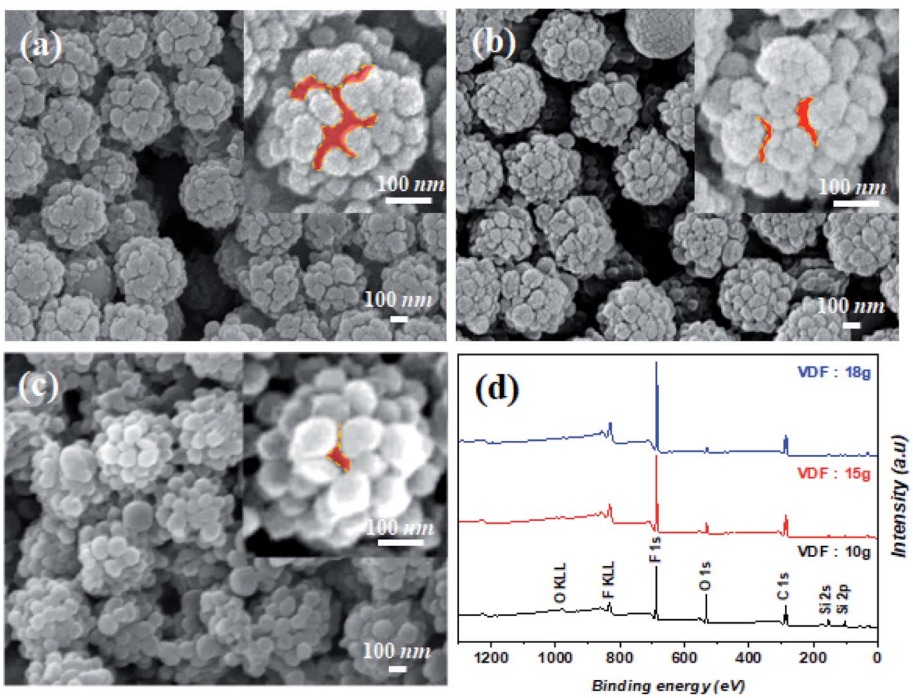

Fig. 2 Preparation and analysis of SPRCSPs according to the amount of VDF gas. SEM and high magnification SEM (insert) images of SPRCSPs prepared using VDF gas: (a) 10 g, (b) 15 g, and (c) 18 g. (d) XPS spectra of SPRCSPs. (red area: core silica area).

explains the presence of some OH groups on the surface of the silica core. Further, by controlling the amount of the VDF precursor, which polymerizes to produce the PVDF coating, the interactions between the core surface and water molecules can be controlled (Fig. 2a–c). In other words, the silica areas that can react with water remain exposed, depending on the degree of PVDF coating. As the reaction progressed, the PVDF coating further grew from the vinyl-modified areas on the silica particles (Fig. 2a; S1a†) eventually connecting with each other (Fig. 2b, c, S1b and c†). Consequently, the area of the unmodified silica with OH groups that can react with water gradually disappeared. Moreover, the amount of F increased with increasing VDF amount, whereas the amount of O and Si concurrently decreased (Fig. 2d). In addition, all the PVDF sub-particles connected with each other as the amount of VDF increased, thereby completely coating the silica surface (Fig. S2†).

3.2 Controllable sticky superhydrophobic structures by SiO2@PVDF raspberry core–shell particles

A spray coating method is generally used to evenly distribute colloidal particles on a substrate and offers the advantages of easy control, low cost, and high efficiency. In addition, it can attain ordered structures.[45,46] Therefore, we spray-coated SPRCSPs onto a substrate using an air spray nozzle (Fig. 3a), which resulted in an ordered arrangement (Fig. 3b). This uniform and ordered coating is suitable for confirming the behavior of water according to the raspberry particle morphology. This is because the changes in the CA can be attributed to the degree and shape of the PVDF shell-coated silica core, and not the overall surface roughness of the structured coating (Fig. 3c).

To that end, the water CAs were measured to confirm the wetting behavior of the structured SPRCSPs coatings synthesized with varying amounts (10–25 g) of the VDF precursor. In general, a smooth surface modified by $-CF_3$ groups (*i.e.*, without any structural ordering) has a CA of 120°, despite its low free energy.[47] PVDF particles with a smooth surface that are not raspberry-shaped exhibit a CA of 117°, owing to the $-CF_3$ functional groups and the colloidal nature of the resultant coating (Fig. S3a and b†). In contrast, the coatings made from SPRCSPs exhibited a larger CA because of the larger empty space between these rough particles than those between conventional smooth particles (Fig. 3d–f). However, in the structured coatings composed of particles with a mitigated raspberry morphology, where the PVDF shell grew smoother and more uniform, the empty space between the particles was reduced, causing a decrease in the CA (Fig. S3c†). In addition, the SPRCSPs have silica cores that influence the wetting properties of the PVDF shell and the resultant structured coating. Furthermore, the amount of the corresponding hydrophilic areas on the water-contacting silica core surface decreased with increasing VDF amount (10–18 g) despite the same raspberry shape; this caused an increase in the CA from 142° to 165° (Fig. 3g). However, when the amount of VDF was increased to 25 g, the raspberry-like structure of the particles weakened, and the CA decreased to 131°.

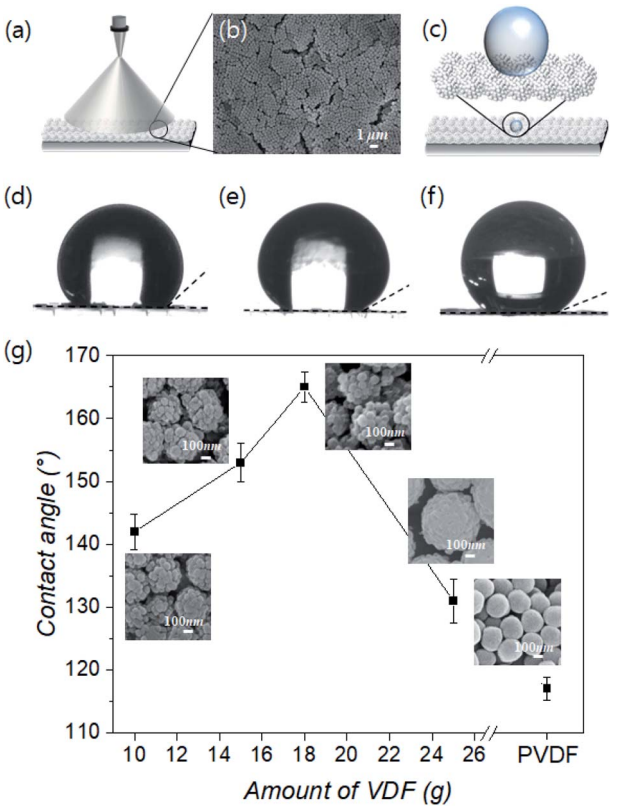

Fig. 3 (a) Schematic of spray coating SPRCSPs onto the substrate. (b) SEM images of the ordered structure of the resulting SPRCSP coating (VDF 18 g). (c) Schematic of a water droplet on the structured coating composed of SPRCSPs. Optical image of the CA between the water droplet and the structured coating composed of SPRCSPs prepared using VDF gas: (d) 10 g, (e) 15 g, and (f) 18 g. (g) Change in the water CA corresponding to the amount of VDF gas used for SPRCSP preparation. Insets: photographs of SPRCSPs corresponding to the different amounts of VDF gas and pure PVDF.

While superhydrophobic structures typically have a CA of 150° or greater without stickiness, a structured coating made of raspberry-shaped particles is sticky even at a CA of 150° or greater. The SPRCSPs (VDF 15 g) prepared by controlling the area of core silica parts exhibited strong stickiness with a high CA of 150° or greater, owing to the hydrophilicity of the core silica (Fig. 4a, Video S1†). The water droplets remained adhered to the coating even at tilting angles of 90° (vertical) and 180° (upside down) (Fig. 4b).

We also measured the effect of applying a centrifugal force to the coated substrate on the CA. The centrifugal force was applied using a spin coater while gradually increasing the rotational speed (500–2000 rpm). Although the CA decreased, a significant portion of the water droplets remained adhered to the structured coating (Fig. 4c). Such strong adhesion can be beneficial for potential applications in water/fog collection systems[48] and microdroplet manipulation.[49] In contrast, SPRCSPs (VDF 18 g) with almost no core silica exposed exhibited weak adhesivity and the water droplets detached from the coated substrate (Fig. 4d, Video S2†). In addition, when a water droplet was dropped onto the SPRCSP (VDF 18 g) structured

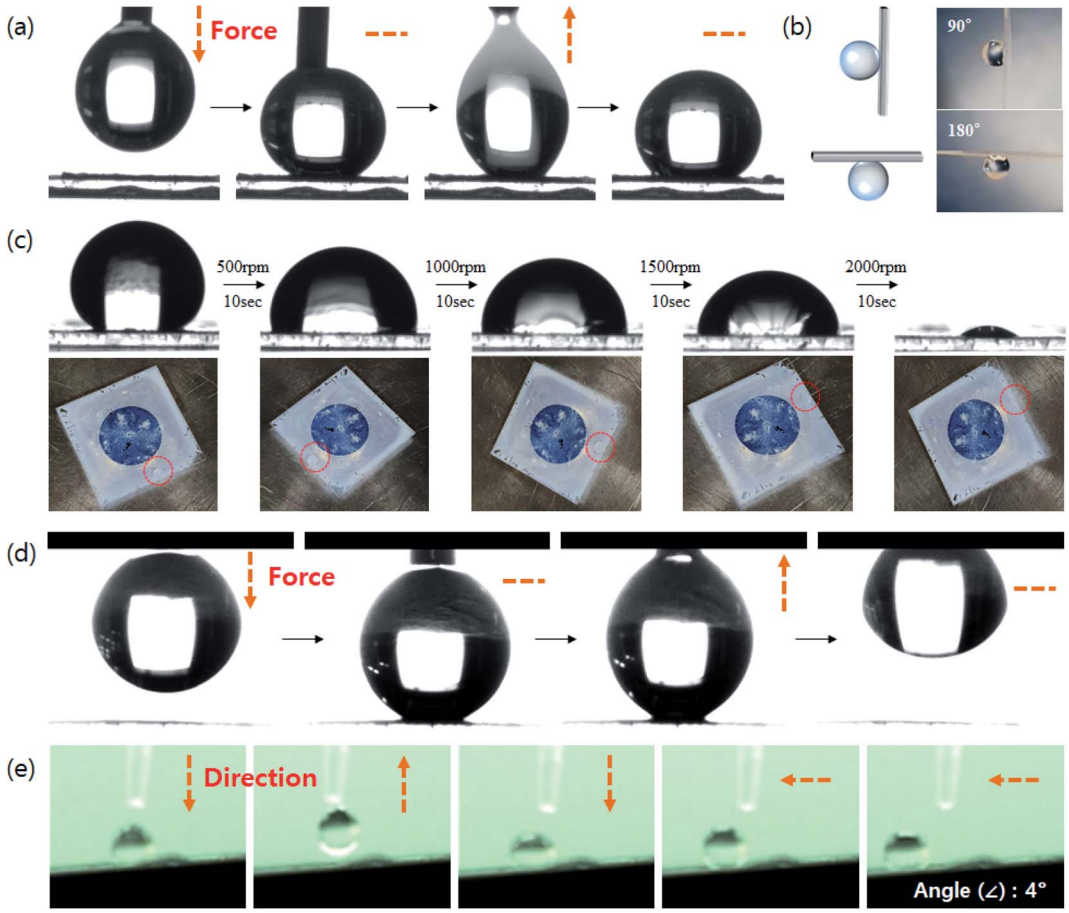

Fig. 4 (a) Dropping water droplet and its movement on a sticky structured coating using SPRCSPs (15 g VDF). (b) Water droplet behavior at 90° and 180° inclination of the sticky SPRCSP coating (VDF 15 g). (c) Water droplet behavior on the sticky SPRCSP coating (VDF 15 g) after applying a rotational force while gradually increasing the rotational speed (500–2000 rpm) for 10 s. (d) Dropping water droplet and its and movement on a low-strength sticky SPRCSP coating (VDF 18 g). (e) Images of the moving water droplet on a SPRCSP coating (VDF 18 g) with a tilting angle of 4°.

coating at a tilting angle of 4°, it bounced on the coating several times and rolled to the bottom (Fig. S4, 4e and Video S3†). This behavior may be beneficial for self-cleaning surfaces.[50]

4. Conclusion

To obtain controllable superhydrophobic structures with strong adhesivity, a new facile strategy was developed for fabricating colloidal structured coatings using SPRCSPs. Raspberry-shaped particles composed of PVDF were specifically synthesized using VDF, a gaseous precursor instead of the conventional liquid precursors. Unlike the conventional method, which requires surface modifications using a fluorine monomer, the current approach resulted in a perfect core–shell form. In addition, the degree of coating of the PVDF shell was controlled to enable interactions between some of the silica, constituting the hydrophilic core, and water molecules. As a result, the superhydrophobicity and stickiness of the structured coating were controllable. The controlled superhydrophobicity led to CAs of 131–165°. For particles with high-strength adhesivity (15 g VDF), the water droplets remained adhered to the substrate even at tilt angles of 90° and 180°. Moreover, when a high centrifugal force was applied, some water droplets maintained their shape. However, for particles with low-strength adhesivity (VDF 18 g), none of the water droplets maintained their shape, and they slid off the surface after bouncing several times on the coating at a tilting angle 4°. Based on these results, we believe that improving the durability of the coated structures will increase the potential for using the controllable stickiness in a variety of applications, such as real water/fog collection systems and self-cleaning surfaces.

Conflicts of interest

The authors declare no competing financial interest.

Acknowledgements

Funding: This research was supported by the KRICT Basic Research Fund (SS2121-30), the Korea Institute of Energy Technology Evaluation and Planning (KETEP) grant funded by the Korea Government Ministry of Trade, Industry, and Energy (Grant No. 20202010100010) and the Korea Evaluation Institute

of Industrial Technology (KEIT) grant by the Korea Government Ministry of Trade, Industry and Energy [Grant No. 20011038]

References

1 X. Feng, L. Feng, M. Jin, J. Zhai, L. Jiang and D. Zhu, *J. Am. Chem. Soc.*, 2004, **126**, 62–63.
2 A. Marmur, *Langmuir*, 2004, **20**, 3517–3519.
3 T. He, X. Liu, Y. Wang, D. Wu, Y. Liu and X. Liu, *Appl. Surf. Sci.*, 2020, **529**, 147017.
4 F. Wang, D. Wang and Z. Guo, *J. Colloid Interface Sci.*, 2020, **560**, 777–786.
5 W. Ma, J. Zhao, O. Oderinde, J. Han, Z. Liu, B. Gao, R. Xiong, Q. Zhang, S. Jiang and C. Huang, *J. Colloid Interface Sci.*, 2018, **532**, 12–23.
6 L. Qiu, Y. Sun and Z. Guo, *J. Mater. Chem. A*, 2020, **8**, 16831–16853.
7 S. Wu, Y. Du, Y. Alsaid, D. Wu, M. Hua, Y. Yan, B. Yao, Y. Ma, X. Zhu and X. He, *Proc. Natl. Acad. Sci.*, 2020, **117**, 11240–11246.
8 T. Mouterde, P. Raux, C. Clanet and D. Quéré, *Proc. Natl. Acad. Sci.*, 2019, **116**, 8220–8223.
9 H. Wang, M. He, H. Liu and Y. Guan, *ACS Appl. Mater. Interfaces*, 2019, **11**, 25586–25594.
10 K. Isakov, C. Kauppinen, S. Franssila and H. Lipsanen, *ACS Appl. Mater. Interfaces*, 2020, **12**, 49957–49962.
11 S. T. Yohe, Y. L. Colson and M. W. Grinstaff, *J. Am. Chem. Soc.*, 2012, **134**, 2016–2019.
12 X. Zhang, L. Wang and E. Levänen, *RSC Adv.*, 2013, **3**, 12003–12020.
13 Y. Lai, Y. Tang, J. Gong, D. Gong, L. Chi, C. Lin and Z. Chen, *J. Mater. Chem.*, 2012, **22**, 7420–7426.
14 Y. Bai, H. Zhang, Y. Shao, H. Zhang and J. Zhu, *Coatings*, 2021, **11**, 116.
15 G. B. Hwang, K. Page, A. Patir, S. P. Nair, E. Allan and I. P. Parkin, *ACS Nano*, 2018, **12**, 6050–6058.
16 Y. Yang, X. Li, X. Zheng, Z. Chen, Q. Zhou and Y. Chen, *Adv. Mater.*, 2018, **30**, 1704912.
17 V. Sharma, K. Yiannacou, M. Karjalainen, K. Lahtonen, M. Valden and V. Sariola, *Nanoscale Adv.*, 2019, **1**, 4025–4040.
18 Y. Wang, H. Lai, Z. Cheng, H. Zhang, Y. Liu and L. Jiang, *ACS Appl. Mater. Interfaces*, 2019, **11**, 10988–10997.
19 S. Zhou, L. Jiang and Z. Dong, *Adv. Mater. Interfaces*, 2021, **8**, 2000824.
20 S. Zhang, J. Huang, Z. Chen and Y. Lai, *Small*, 2017, **13**, 1602992.
21 X. Wang, J. Zeng, J. Li, X. Yu, Z. Wang and Y. Zhang, *J. Mater. Chem. A*, 2021, **9**, 1507–1516.
22 X. Wang, J. Zeng, X. Yu and Y. Zhang, *J. Mater. Chem. A*, 2019, **7**, 5426–5433.
23 Y. Zheng, C. Zhang, J. Wang, Y. Liu, C. Shen and J. Yang, *J. Colloid Interface Sci.*, 2019, **557**, 737–745.
24 J. Cao, D. Gao, C. Li, X. Si, J. Jia and J. Qi, *ACS Appl. Mater. Interfaces*, 2021, **13**, 5834–5843.
25 S. Liu, H. Zhou, H. Wang, Y. Zhao, H. Shao, Z. Xu, Z. Feng, D. Liu and T. Lin, *Adv. Mater. Interfaces*, 2017, **4**, 1700027.
26 X. Zhao, D. S. Park, J. Choi, S. Park, S. A. Soper and M. C. Murphy, *J. Colloid Interface Sci.*, 2021, **585**, 668–675.
27 R. Tan, H. Xie, J. She, J. Liang, H. He, J. Li, Z. Fan and B. Liu, *Carbon*, 2019, **145**, 359–366.
28 A. Baldelli, J. Ou, D. Barona, W. Li and A. Amirfazli, *Adv. Mater. Interfaces*, 2021, **8**, 1902110.
29 L. Zhang, L. Sun, Z. Zhang, Y. Wang, Z. Yang, C. Liu, Z. Li and Y. Zhao, *Chem. Eng. J.*, 2020, **394**, 125008.
30 L. D. C. Castro, N. M. Larocca and L. A. Pessan, *Langmuir*, 2021, **37**, 124–131.
31 M. Nosonovsky and B. Bhushan, *Philos. Trans. R. Soc., A*, 2016, **374**, 20160185.
32 A. K. Kota, G. Kwon and A. Tuteja, *NPG Asia Mater.*, 2014, **6**, e109.
33 Y. Wang, Y. Yang, J. Yuan, M. Pan, G. Liu, H. Ding and C. Ma, *Ind. Eng. Chem. Res.*, 2017, **56**, 7207–7216.
34 H. Yan, X. Lu, C. Wu, X. Sun and W. Tang, *J. Membr. Sci.*, 2017, **533**, 130–140.
35 S. Gao, S. Song, J. Wang, S. Mei, J. Yuan, G. Liu and M. Pan, *Colloids Surf., A*, 2019, **577**, 360–369.
36 X. Zhao, M. Sun, Y. Duan and H. Hao, *Colloids Surf., A*, 2020, **602**, 125039.
37 E.-H. Sohn, H. S. Kang, J.-C. Bom, J.-W. Ha, S.-B. Lee and I. J. Park, *J. Mater. Chem. A*, 2018, **6**, 12950–12955.
38 J. Lee, H. S. Hwang, T. N. H. Lo, W.-G. Koh and I. Park, *Polymers*, 2020, **12**, 2864.
39 C. Chen, L. Zhang, M. Sheng, Y. Guan, H. Dong and S. Fu, *J. Mater. Sci.*, 2019, **54**, 1898–1912.
40 D. Xu, M. Wang, X. Ge, M. Hon-Wah Lam and X. Ge, *J. Mater. Chem.*, 2012, **22**, 5784–5791.
41 E. Bourgeat-Lami and M. Lansalot, *Adv. Polym. Sci.*, 2010, **233**, 53–123.
42 Y. Li and B. Liu, *ACS Macro Lett.*, 2017, **6**, 1315–1319.
43 K. Zhang, H. Chen, X. Chen, Z. Chen, Z. Cui and B. Yang, *Macromol. Mater. Eng.*, 2003, **288**, 380–385.
44 L. Feng, Y. Zhang, J. Xi, Y. Zhu, N. Wang, F. Xia and L. Jiang, *Langmuir*, 2008, **24**, 4114–4119.
45 L. Cui, Y. Zhang, J. Wang, Y. Ren, Y. Song and L. Jiang, *Macromol. Rapid Commun.*, 2009, **30**, 598–603.
46 C. Wang, X. Lin, C. G. Schäfer, S. Hirsemann and J. Ge, *Adv. Funct. Mater.*, 2021, **31**, 2008601.
47 T. Nishino, M. Meguro, K. Nakamae, M. Matsushita and Y. Ueda, *Langmuir*, 1999, **15**, 4321–4323.
48 J. Knapczyk-Korczak, P. K. Szewczyk and U. Stachewicz, *RSC Adv.*, 2021, **11**, 10866–10873.
49 L. Wang, Y. Tan, K. Gan, L. Liu, X. Chen, M. Tang, B. Hu and W. Wu, *Langmuir*, 2021, **37**, 4129–4136.
50 Y. Luo, S. Wang, X. Fu, X. Du, H. Wang, X. Cheng and Z. Du, *RSC Adv.*, 2021, **11**, 4660–4671.